

Design, manufacturing and operation of a small turbojet-engine for research purposes

Ernesto Benini ^{*}, Stefano Giacometti

Dipartimento di Ingegneria Meccanica, Università di Padova, Via Venezia, 1 – 35131 Padova, Italy

Available online 27 July 2007

Abstract

A research project is on going, at the University of Padova, to develop a 200 N static-thrust engine to be used for both didactic and research activities. This paper describes in detail all the phases required to set-up such an engine, including design, manufacturing and operation. The jet engine features a single-stage centrifugal compressor developing 2.66:1 compression ratio at 60,000 rpm, a direct-flow annular combustion chamber and a single-stage axial turbine with 950 K turbine-inlet temperature (TIT). All the design and manufacturing details are provided, as well as the operation procedure together with experimental results.

© 2007 Elsevier Ltd. All rights reserved.

Keywords: Small turbojet; Turbojet engine; Design; Operation; Combustion

1. Introduction and background

During recent years, interest on small-sized gas-turbine engines has increased for both ground-based and vehicular uses. Small-size turbojet engines, in particular, are becoming attractive for their potential application on remote-control airplanes or on unmanned aerial vehicles (UAVs) because of their extremely-high thrust-to-weight ratio [1]. A number of small turbojet design examples are available that develop less than 200 N static thrust (e.g. [2,3]) which have been derived from large turbojet scale-down procedures, but at a micro scale [4]. However a deep understanding of the behaviour of these engines is far from being ascertained.

^{*} Corresponding author. Tel.: +39 049 8276767; fax: +39 049 8276785.

E-mail address: ernesto.benini@unipd.it (E. Benini).

The lack of knowledge involves almost all the phases of the engine set-up and development: design, manufacturing, operation and testing of small engines are regulated by different concepts rather than large aircraft propulsors and require tailored procedures.

The design of such machines is inevitably influenced by their small size. For a millimetre/centimetre-scale gas turbine [5], designers have to deal with engineering challenges comparable with those which characterize large conventional machines, plus the fact that traditional design criteria do not necessarily apply in the new design space. This involves particularly the aero-thermo-mechanical behaviour of engine components, since the thermodynamic cycle is characterized by relatively high operating temperatures, very low component pressure-ratios and efficiencies, and high rotational speeds of the core-assembly. In this context, the role played by the low Reynolds numbers on engine performance is significant and indicates the dominance of frictional forces over inertial ones. Also, heat-transfer related problems due to the compact engine may affect the engine design and choice of core-engine architecture. The result is the necessity of an accurate aero-thermo-dynamic design and, ultimately, a very sensitive engine in terms of operation and off-design behaviour.

Moreover, combustion-related problems are huge, especially in terms of flame stabilization. This involves an accurate design of the combustion chamber and the set-up of an efficient recirculation within the combustion primary zone.

Also manufacturing aspects are peculiar to these engines because of their small size. Components rotate at very high velocities ($>30,000$ rpm) so that balancing becomes decisive for safe and durable operation. This implies rotating parts to be machined with very high precision. The use of bearings featuring excellent stiffness and damping properties is therefore of primary importance.

The University of Padova is undergoing a project aimed at developing small turbojet engines for research and educational purposes. The ultimate goal of this project is to acquire the necessary competency to design, manufacture, operate and test such engines.

2. Design specifications

When defining the specifications for the turbojet engine, we thought about a compact, lightweight and possibly low-cost system that was able to develop approximately 200 N thrust under ISO conditions, a choice that we identified as reasonable for an effective research/didactic experiment without excessive expenditure regarding the propulsor and the test bench. These features were achieved according to some basic thermodynamic and mechanical rules, described as follows:

1. Select a simple open Brayton–Joule thermodynamic cycle in order to make the overall design and system architecture as simple as possible, and thus avoid any cycle sophistication, such as internal regeneration, air bleeding, blade cooling, etc.
2. Adopt a turbine-inlet temperature smaller than 1000 K. Even if this choice limits the maximum obtainable thermal efficiency to values less than 20% (when the engine is operated at sea-level conditions), it makes it possible to use a low-cost steel to construct the turbine parts.
3. Choose a single-shaft configuration. Such a characteristic has a positive impact on engine weight and size, as well as on component simplicity, although it makes the engine less flexible in its operation.

4. Use standard-technology turbomachinery and rotordynamics design, without any variable geometry device and using standard ball-bearings to support the core engine.
5. Use an exhaust nozzle having convergent shape so that the flow is always subsonic at the engine's exhaust, except when the engine operates in choking condition.

3. Design procedure of the turbojet engine

The following are the steps that we followed in the development of the turbojet.

3.1. Thermodynamic-cycle design and analysis

A Brayton–Joule cycle simulator was used to predict the performance of the turbojet engine; the simulator was implemented as described in detail in [6]. In the thermodynamic model, the following assumptions were made:

- Ambient pressure and temperature of air are 288.15 K and 101.3 kPa, respectively.
- Air behaves as an semi-ideal gas with specific heats variable with temperature.
- Fuel/air mixture behaves like a semi-ideal equivalent gas with enthalpy, entropy and specific heats depending on temperature and fuel/air equivalence ratio [7].
- Intake isentropic-efficiency is 0.97.
- Compressor's isentropic-efficiency is 0.78.
- Burner efficiency is 0.94.
- Combustor's pneumatic-efficiency is 0.9.
- Turbine's isentropic-efficiency is 0.8.
- Nozzle's isentropic-efficiency is 0.98.
- Nozzle is unchoked.

The fuel is assumed to be liquid kerosene for residential use with a heating value of 42,700 kJ/kg.

Using such hypotheses, a parametric analysis was carried out to derive the cycle pressure ratio that guaranteed the maximum engine specific thrust of 377 N/(kg/s). Therefore, a pressure ratio of 2.66 was selected and a maximum cycle-temperature of 950 K was adopted accordingly. Correspondingly, for the design thrust of 200 N at the fixed point, the air mass flow rate is 0.53 kg/s. The other relevant parameters of the cycle are reported in Table 1.

3.2. Compressor design

For small, compact and light-weight jet engines, the choice of a single-stage centrifugal compressor featuring a double-stage diffuser (radial and deswirl) is mandatory [8]. Using the design data from the cycle study, the impeller and diffuser were designed following the procedure outlined by [8,9]. For the sake of simplicity, we decided to design an impeller with radial blades, because, this typology easier to be manufactured, even if it is recognized not to be as optimal as a backswept-bladed impeller [8,10,11] as far as the peak efficiency and part-load operation are concerned.

The first step consisted in a one-dimensional calculation of the impeller and the diffuser, including loss and deviation correlations provided by Aungier [13].

Table 1

Relevant parameters at fixed-point operation from the cycle analysis

Required static thrust at ISO conditions	200 N
Turbine's inlet temperature (TIT)	950 K
Compression ratio	2.66
Compressor's delivery-pressure	262 kPa
Compressor's delivery-temperature	407 K
Turbine's inlet-pressure	246 kPa
Turbine's outlet-pressure	137 kPa
Turbine's outlet-temperature	847 K
Fuel/air ratio	0.0137
Specific thrust	377 m/s
Nominal speed	60,000 rpm
Thermal efficiency	12%

Next, a three-dimensional model of the compressor was implemented and simulated using a Navier–Stokes solver (Ansys CFX 10©), where a “stage” interface between the impeller and diffuser was adopted during the calculations [12], an excerpt of which is reported in Fig. 1. The simulations predicted the values for the compression ratio and isentropic efficiency, which were different from those adopted in the first-cycle analysis. Therefore, a new simulation of the engine cycle was carried out and a redesign of the compressor was performed accordingly. This procedure was repeated until convergence from cycle analysis and component performance was successfully achieved. The finally designed compressor (Figs. 2 and 3) featured an impeller with 20 radial blades (including 10 splitter blades for improving the flow guidance at part-load operation), an outer diameter of 129 mm, an inlet diameter of 74 mm and a tip speed at the design point (60,000 rpm) of 405 m/s. The downstream diffuser features 19 radial and 38 deswirl blades, the latter being designed to provide an axial flow of air without too much swirl in the combustion chamber (the amount of swirl must be contained in the portion from the compressor impeller exit to the combustion chamber inlet so as not to introduce excessive pressure losses herein).

The predicted maps of the compressor are illustrated in Fig. 4.

The compressor impeller was obtained from one piece of Aluminium Alloy (Ergal) using a 5-axis numerical control machine. The diffuser was constructed in the same way from a piece of magnesium. The compressor casing was finally obtained from forged magnesium.

A typical bell-mouth-shaped intake was used in this engine for assuring good inlet flow characteristics for the compressor, as static thrust is to be developed [14]. The intake and compressor casing are two separate items made of an aluminium alloy. The machining of the rotor casing had to be highly accurate. Large tip clearances are detrimental to overall engine performance and compressor efficiency, especially with small inlet diameters. Tip clearances have been kept around 0.2 mm, the minimum practical for radial and axial rotor displacement control and alignment.

3.3. Combustion-chamber design

As one might expect, the combustion chamber design is a very complicated task in small gas-turbine engines, being its size limited by the strong coupling issues regarding the compressor and turbine, typically constructive limitations on shaft length and diameter. These

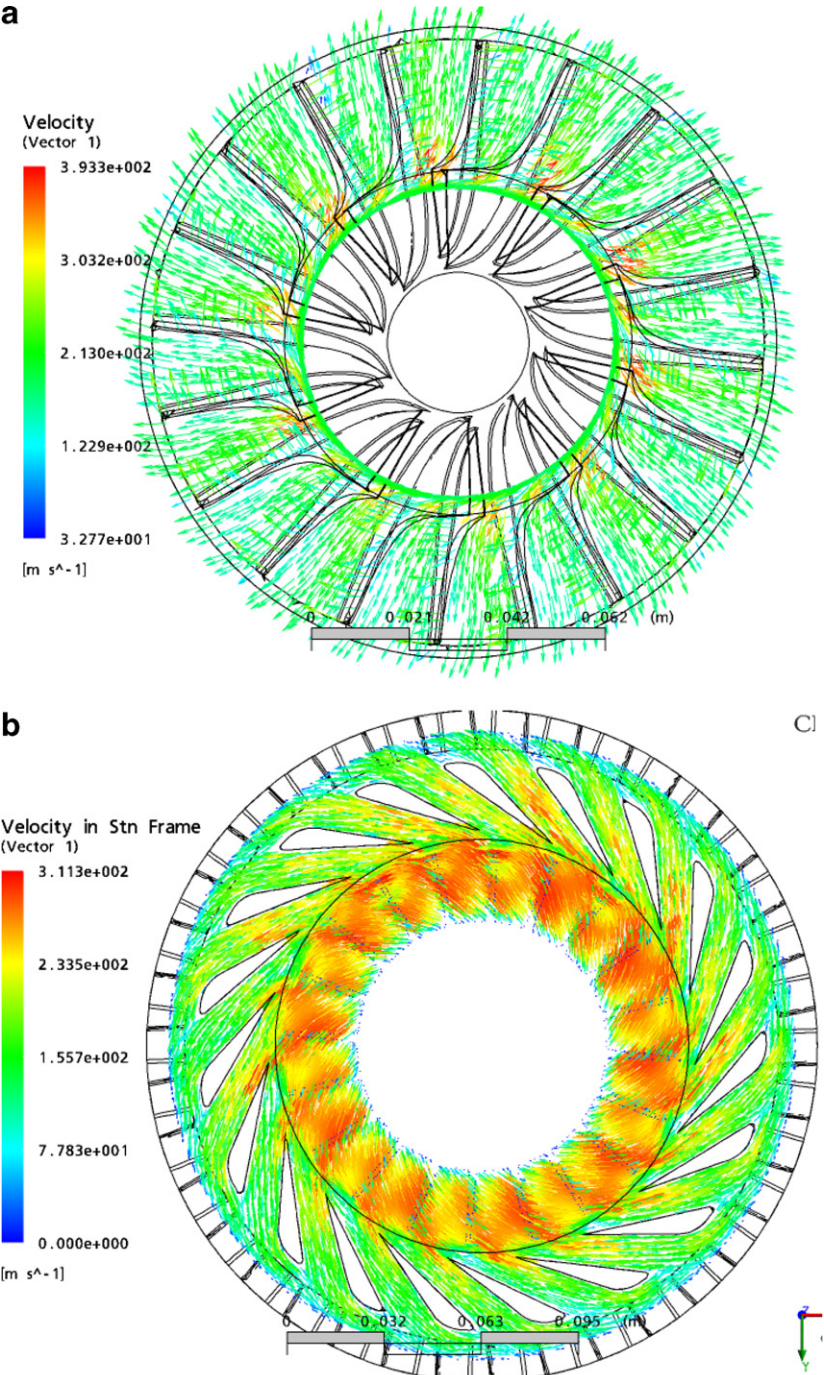


Fig. 1. Velocity field in (a) the impeller and (b) diffuser obtained from the CFD simulation of the compressor at 60,000 rpm.

requirements have focused our attention on a particular type of combustor, i.e. a direct-flow annular chamber. This layout is illustrated in Figs. 5, 6 and 10: the air exiting the compressor is subject to quite a sudden diffusion within the gap between the compressor diffuser outlet and the combustor liner, and then directly forced to enter the chamber

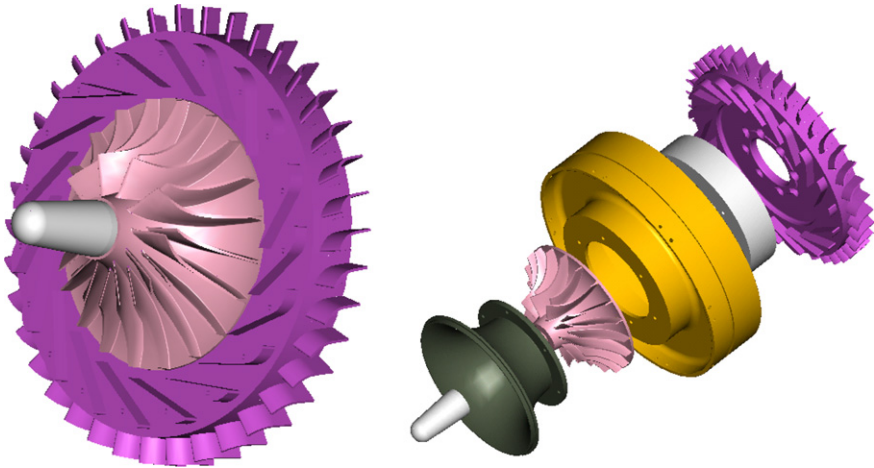


Fig. 2. Computer representation of the compressor assembly.



Fig. 3. Photos of the manufactured compressor.

though circumferential holes (therefore without the use of a swirler), where it mixes with the evaporated fuel that impinges against the air stream from the cylindrical fuel injector pipes. The mixing is augmented by the presence of turbulators, and the recirculation in the

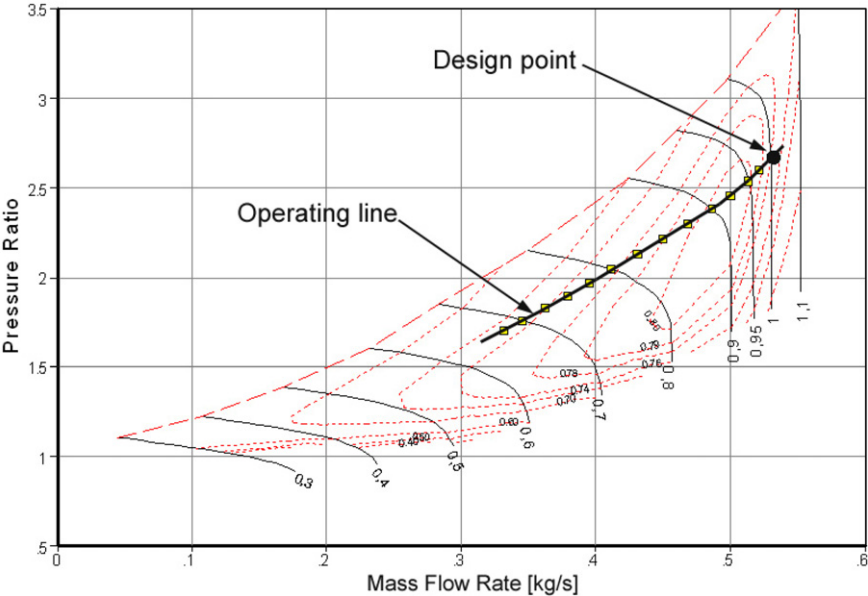


Fig. 4. Predicted compressor map.

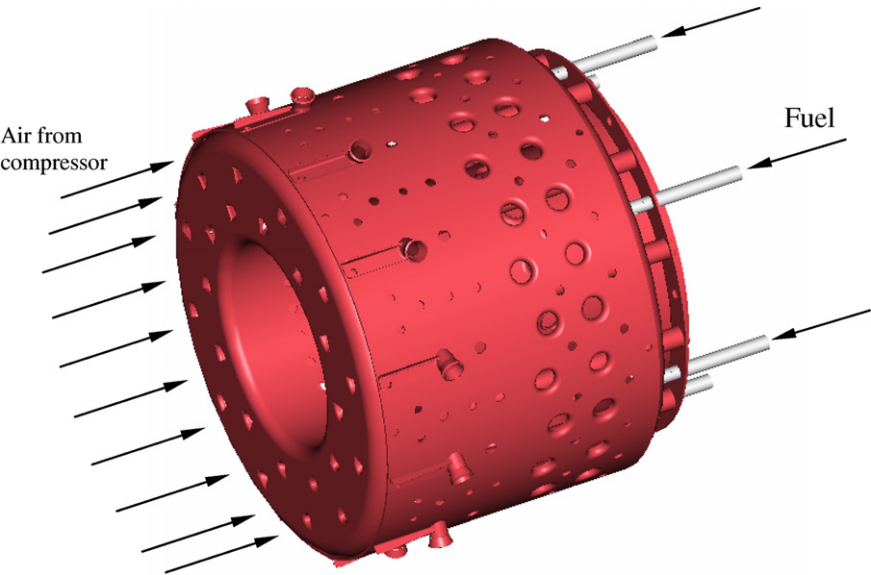


Fig. 5. Computer representation of the combustion-chamber.

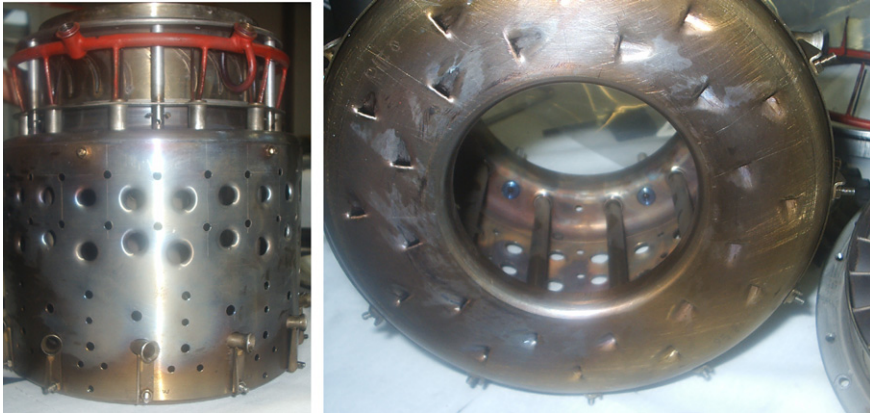


Fig. 6. Photos of the constructed combustion chamber.

primary zone is created from the interaction between the primary air entering the combustor front and the air jets entering from outside the liner.

The main advantages of this configuration are similar to those characterizing the traditional annular combustion chamber of large-size engines [15]: satisfactory fuel–air mixing, compactness, lightness, and efficient liner cooling. In fact, this arrangement does not exhibit excessive surface-to-volume ratio of the liner, as in reverse-flow combustors. However, the main drawback is the relatively poor aerodynamic performance due to the high pressure-loss that occurs in the diffusion zone.

The design of the combustor was performed following the rules dictated by Lefebvre [15]: Two main issues have been considered and lead to a complicated design, i.e. a correct primary-zone recirculation and the problem of flame stabilization.

The so-called swirl vanes at the entry to the combustor, a solution which is widely used in large gas-turbines, were not used because of difficulties in manufacturing and because fuel was not intended to be injected by means of individual nozzles. Instead, large-scale primary-zone recirculation using a small number of large air jets has finally led to the successful design. When correctly placed, these recirculation holes significantly improved mixing and combustion stability, and the test runs resulted in a spotless combustion chamber.

Regarding flame stability, some issues deserve to be discussed. As is well known, stability limits for sustained combustion with respect to fuel-to-air ratio are wide, but these limits are much narrower for ignition. Therefore, good ignition characteristics depend greatly on the fuel-injector design and the achievable atomization quality. A well-atomized or evaporated fuel (preferably close to the stoichiometric fuel-to-air ratio) is required in the primary zone, especially at low rotational speeds, when air temperature and pressure at the inlet to the combustion chamber are almost ambient. This is especially detrimental to ignition performance because of the large ignition heat-loss and the very poor fuel-atomization quality that can actually be achieved.

High-quality fuel atomization using plain orifice nozzles was investigated, but small high-performance orifice nozzles require high fuel-pressures and heavy onboard boost-pumps to achieve fine fuel-sprays. Moreover, they tend to create large spray-cone angles, and a finer fuel spray will mean a larger cone angle. The heat transfer caused by the impingement of burning droplets onto the liner's inner wall is high, especially in a very

small combustion chamber. For these reasons, fuel pre-evaporation provided the best solution. The design consists of a fuel pre-evaporator manifold located within the combustion chamber. Because the fuel and the combustion chamber are cold at start-up, the fuel cannot be pre-evaporated unless it is preheated to its high evaporation temperatures just before ignition, which is cumbersome. The solution was to use a natural-gas fuel for start-up and ignition. The latter was accomplished by a discharge spark-ignition unit developed in-house.

A kerosene fuel was then selected for operating this turbojet engine after start-up. At minimum idle speed, the transfer to kerosene fuel is initiated through the same gas manifold, using synchronized valves. The already hot gases in the combustion chamber then preheat the fuel in the manifold to a high evaporation level before it enters the combustion chamber. Kerosene has good combustion characteristics when properly *evaporated* and is much safer to handle than gasoline or liquefied petroleum gas. Although very flammable, kerosene has less of a tendency to form explosive mixtures quickly when a leak occurs, such as from pumps or feed lines. Safety in fuel handling and engine operation has been a serious design issue. Finally, since kerosene at high temperatures tends to produce coke as a result of the thermal cracking of hydrocarbons, we were particularly worried about coke layer formation on the inner wall of the evaporators.

The use of kerosene did require the addition of a booster pump for fuel pressurization. The main difficulty with kerosene fuel was proper evaporation within the limited space of the combustion chamber. Ample margins in temperature (thermal stress) and rotor speed (component loadings) have been provided to ensure a long life, particularly for the hot-section components. The maximum operating turbine-inlet temperature of 1000 K has proven to be well below the turbine's capability. The constructed combustion chamber (using AISI 316L steel) is depicted in Fig. 6.

3.4. Turbine design

As a result of the combustion chamber design, and therefore from a knowledge of the fluid/mass flow rate to be expanded, as well as the fluid's stagnation-temperature and pressure at the combustor exit, a single-stage, axial-flow turbine was selected as the preferred configuration to drive the compressor. It consists of a nozzle row and a 0.55 reaction turbine wheel. The profiles of the nozzle and the rotor are in-house evolutions of the standard A₃K₇ airfoils that we studied to obtain satisfactory performance from both the aerodynamic and structural points of view. They were actually derived using a prescribed-curvature turbine-blade method [19].

The preliminary design was carried out using a one-dimensional procedure at the mean radius of the turbine, following the well-known procedure illustrated by Horlock [18], and using loss correlations given by Craig and Cox [17], and the deviation correlation expressed by Ainley and Mathienson [20]. The nozzle row featured 25 blades having constant stagger angles with radius, while a free-vortex criterion was used to determine the angles at various radii of the 29 rotor blades (Fig. 7). The optimal solidity of each blade row was found using the Zweifel criterion, however setting the tangential-lift coefficient to 1.1, as suggested in [16]. In this way, the loading on the blade was increased with respect to conventional design practice.

The nozzle blade row was constructed using refractory steel 310S. On the other hand, the material used for turbine rotor blades is a W302 steel (both components are

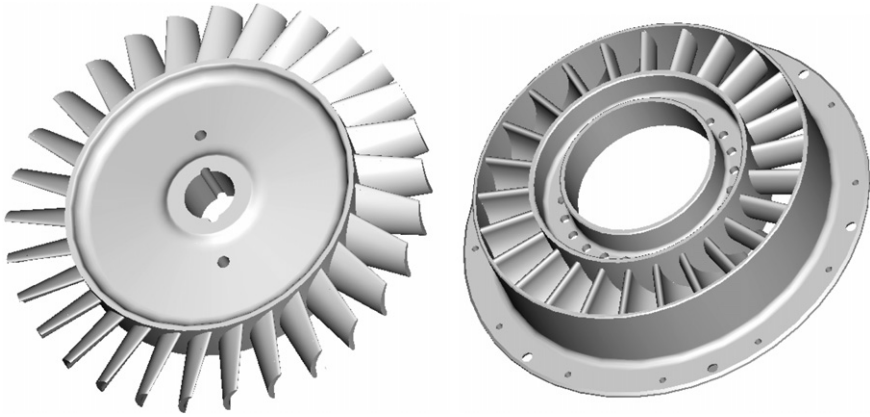


Fig. 7. Computer representation of the turbine rotor (left) and nozzle vanes (right).

represented in Fig. 8). The compressor and turbine are connected using a V145 steel shaft supported by a couple of preloaded ball bearings. The rotor-bearing module was accurately aligned and balanced with all other components in order to control the tip clearances of both compressor and turbine.

Both bearings are lubricated and cooled with oil fed from the externally-mounted tank by a tube through the compressor casing. This lube-oil system is of the total-loss type.



Fig. 8. Photos of the manufactured turbine.

Only a little oil is required during normal operation. A closed-loop system would be too heavy and too difficult to engineer, and would require an overly complex sealing arrangement. The lube-oil flow is controlled by a small orifice of proprietary size, and the oil is fed to both bearings using compressor discharge air. Before start-up, when no pressure is available, oil is fed manually. All oil is finally lost in the exhaust duct where it is entrained in the hot gases.

3.5. Nozzle design

A simple convergent-shaped exhaust nozzle was designed featuring an effective exit area of 6013 cm^2 , which makes the nozzle unchoked at the design point. This component was built from AISI 316L steel plates, and manufactured as illustrated in Fig. 9.

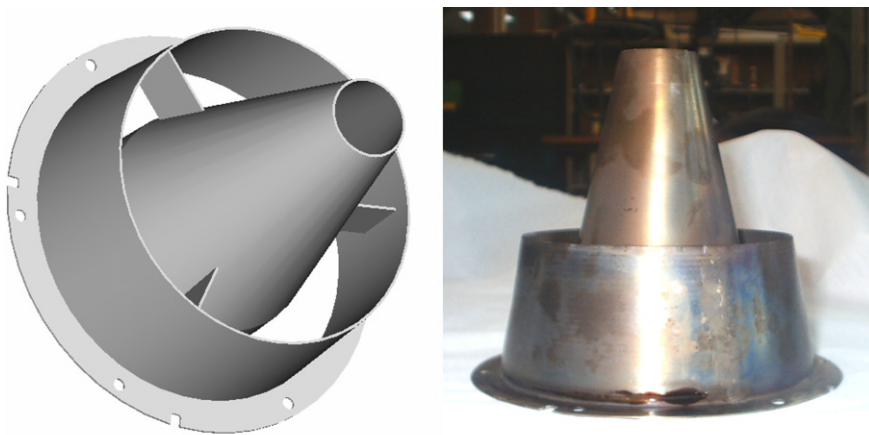


Fig. 9. Discharge nozzle: Computer representation (left) and manufactured component (right).

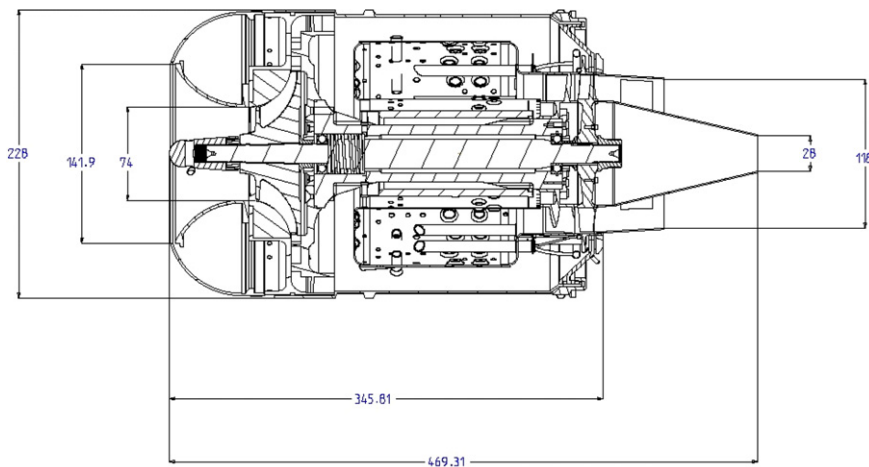


Fig. 10. Two-dimensional drawing of the designed turbojet (dimensions in mm).

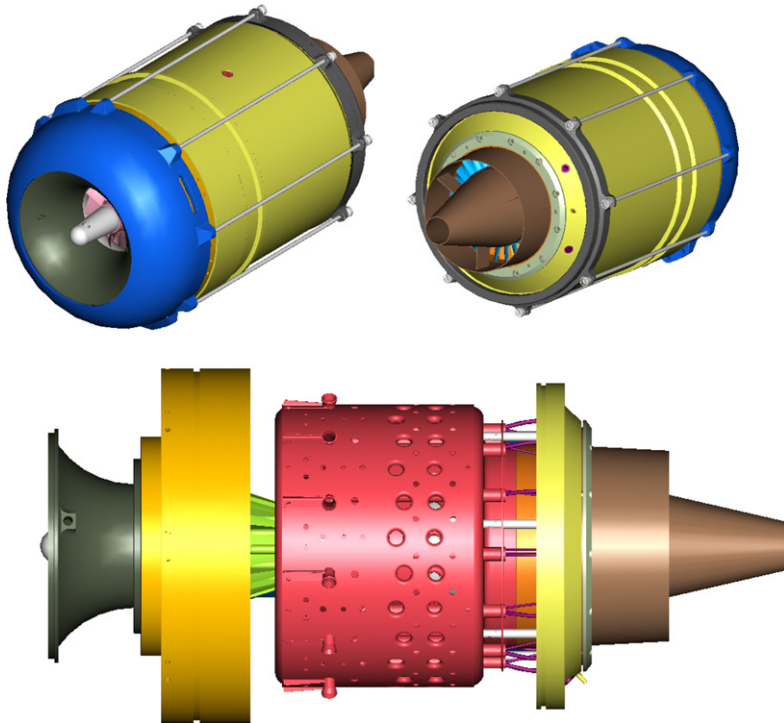


Fig. 11. Computer representation of the designed turbojet.

3.6. Assembly Design

A modular design concept has been maintained throughout the entire engine. All components have been designed to be easily manufactured and assembled. The turbojet engine has been divided into several modules that are combined by means of bolts, press-fit connections, and special clamps. Figs. 10 and 11 show a meridional section and a three-dimensional view of the assembly.

4. Turbojet testing

The developed turbojet, after an accurate balancing of the core-assembly, was mounted and tested on a test rig, whereby rotational speed, exhaust static temperature of hot gases, compressor static discharge pressure, thrust (static), bearing and oil temperature, and fuel pressure and temperature can be measured.

4.1. Test rig and instrumentation

The test rig consisted of a bench where the engine is mounted as depicted in Fig. 12. The test rig is equipped with the following instrumentation:

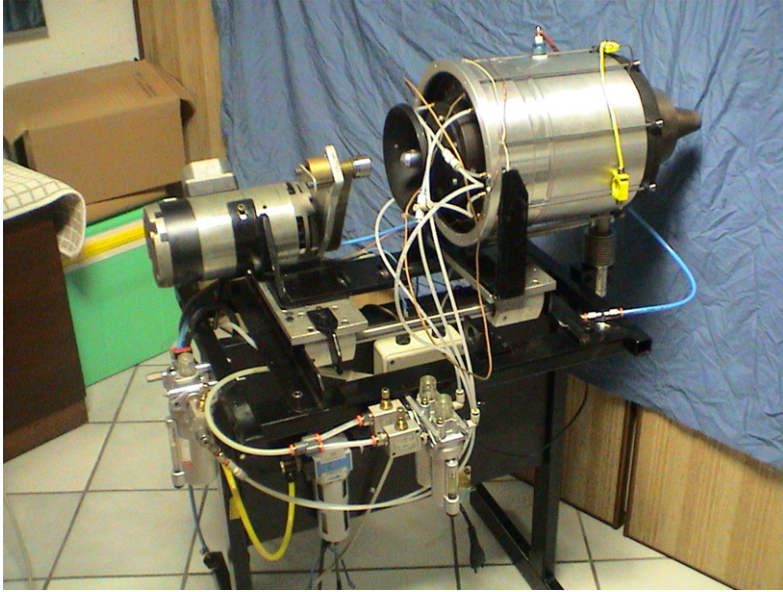


Fig. 12. The turbojet mounted on the test rig.

- (1) Three insulated thermojunctions of the K-type, which are placed downstream of the turbine rotor.
- (2) An analogic Bourdon-type manometer, connected to static-pressure taps place at the compressor outlet.
- (3) A load cell for measuring the thrust developed by the engine.
- (4) A magnetic tachometer, via which the rotational regime of the engine can be measured.
- (5) A volumetric gear pump for pumping the fuel into the combustion chamber.
- (6) An electric motor for starting the engine (i.e. until self-operation is achieved).
- (7) A discharge spark-ignition unit for the igniter.
- (8) Synchronized control valves for both natural-gas fuel and kerosene.
- (9) An *oil pump* for the lubrication of the bearings.

4.2. Test procedure and results

At engine start-up, electric power from the auxiliary motor is used to accelerate the core-assembly to approximately 10,000 rpm.

At this point the ignition is turned on, the natural-gas-fuel valve is opened, and light-up occurs, accelerating the engine further to its minimum idle speed of approximately 20,000 rpm. From this point the electric motor is disconnected and the engine is self-operated. The thrust then produced can be quite easily controlled by acting on the fuel flow rate, which in turn determines the instantaneous rotational velocity of the turbojet.

Changeover from natural-gas fuel to kerosene is accomplished using the same fuel manifold system, by simultaneously closing the gas-fuel valve and opening the liquid-fuel valve. During changeover, the turbojet engine runs on a mixture of gas fuel and kerosene

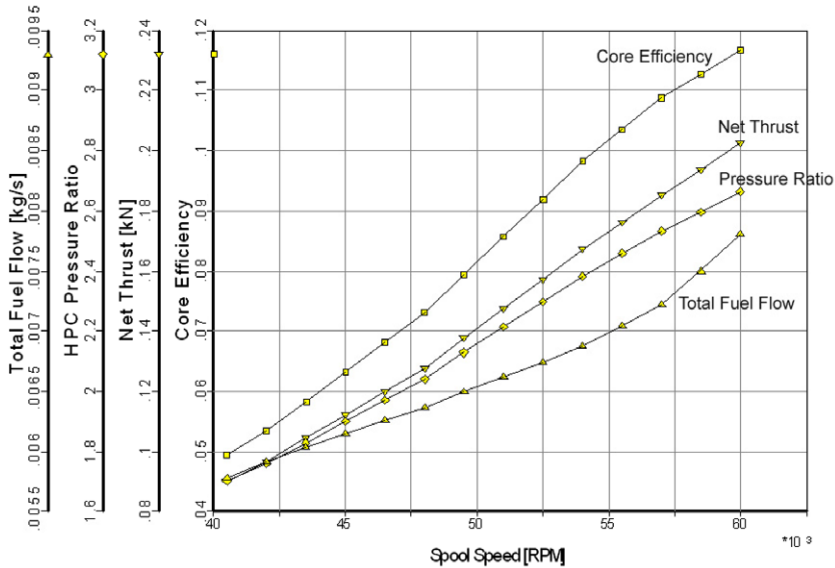


Fig. 13. Performance test results.

for a few seconds. This method has been very successful. Further acceleration to the engine's maximum continuous speed of 60,000 rpm can then be initiated.

The main results of the tests (Fig. 13) are the curves that relate the static net thrust produced, the total fuel consumption, the static compression ratio and the thermal efficiency (also called core efficiency) to the engine's rotational speed.

At present, the engine has undergone over 500 h of operation and performed well without a decrease in performance; moreover we did not register any coke formation on the evaporator walls, but further long-term performance tests have to be carried out to analyze the combustor behaviour over time.

5. Conclusions and future investigations

A large amount of research has been carried out at the Dept. of Mechanical Engineering, University of Padova to design and develop a small, low-cost 200 N-thrust jet engine that can be used for research and didactic purposes. The project made it possible to acquire the necessary expertise to self-design, manufacture, operate and test such engine, and laid the basis upon which further research work can be carried out. In fact, the next steps will be directed toward improving engine efficiency through an increment of cycle pressure ratio and turbine inlet temperature (for which the use of super Nickel alloys and/or ceramic materials is mandatory), followed by endurance and reliability tests.

References

- [1] Chu HH, Chiang Hsiao-Wei. Aerospace technology development – Small gas-turbine development. Taiwan, ROC: Aerospace Development Planning, National Science Council; 1996. p. 4–22.

- [2] Jackson AJB, Laskaridis P, Pilidis P. Test bed for small aero gas-turbines for education and for University–Industry Collaboration. ASME Paper GT-2004-54334; 2004.
- [3] Davison CR, Birk AM. Set-up and operational experience with a micro-turbine engine for research and education. ASME Paper GT-2004-53377; 2004.
- [4] Epstein AH. Millimeter-scale, MEMS gas-turbine engines. ASME Paper GT-2003-38866.
- [5] Rodgers C. Some effects of size on the performances of small gas-turbines. ASME Paper GT-2003-38027; 2003.
- [6] Hill PG, Peterson CR. Mechanics and thermodynamics of propulsion. Reading (MA): Addison-Wesley; 1992.
- [7] Cumpsty N. Jet propulsion. Cambridge: Cambridge University Press; 1997.
- [8] Japikse D. Centrifugal-compressor design and performance. Wilder, Vermont: Concepts ETI, Inc.; 1994.
- [9] Whitfield A, Baines NC. The design of radial turbomachines. London, UK: Longman; 1990.
- [10] Zangeneh M, Goto A, Harada H. On the design criteria for suppression of secondary flows in centrifugal and mixed-flow impellers. ASME J Turbomachinery 1998;120:723–35.
- [11] Benini E. Optimal Navier–Stokes design of compressor impellers using evolutionary computation. Int J Comput Fluid Dyn 2003;17(5):357–69.
- [12] Benini E, Toffolo A, Lazzaretto A. Experimental and numerical analyses to enhance the performance of a microturbine diffuser. Exp Thermal Fluid Sci 2006;30(5):427–40.
- [13] Aungier RH. Centrifugal compressors – A strategy for aerodynamic design and analysis. New York: ASME Press; 2000.
- [14] Cumpsty NA. Compressor aerodynamics. UK: Longman Group; 1989.
- [15] Lefebvre AH. Gas-turbine combustion. 2nd ed. London: Taylor & Francis; 1999.
- [16] Wilson DG, Korakianitis T. The design of high-efficiency turbomachinery and gas turbines. 2nd ed. Englewood Cliffs (NJ): Prentice-Hall; 1998.
- [17] Craig HRM, Cox HJA. Performance prediction of axial-flow turbines. Proc Inst Mech Engrs 1971;185(32/71).
- [18] Horlock JH. Axial-flow turbines. London: Butterworths; 1966.
- [19] Korakianitis T. Prescribed-curvature-distribution airfoils for the preliminary geometric design of axial-turbomachinery cascades. J Turbomachinery 1993;115(2):325–33.
- [20] Ainley DG, Mathienson GCR. An examination of the flow and pressure losses in blade rows of axial-flow turbines R&M No. 2892 (March). UK: Aeron. Research Comm.; 1951.